Identification of natural organic matter (NOM) transport behavior near the membrane surface using flow field-flow-fractionation (fl-FFF) micro channel

Do Hee Kim, Jihee Moon and Jaeweon Cho

ABSTRACT

Membrane fouling due to natural organic matter (NOM) is a major obstacle in the membrane filtration process for water treatment and water reuse facilities. Flow field-flow-fractionation (fl-FFF) is capable to evaluate interactions between NOM and the membrane surface in terms of size exclusion, electrostatic interaction and reversible/irreversible adsorption, as well as NOM characterisations. The effects of the membrane surface charge and ionic strength on the behavior of polystyrene sulfonates (PSS) and NOM in membranes were demonstrated using fl-FFF. Membrane fouling due to NOM adsorption on the membrane surface was investigated by, and correlated to, fl-FFF. Ionic strength had an effect on both the structure of PSS or NOM and the membrane matrix so that different retention peaks were observed. It also affected the interaction between membrane and solute, and resulted in solute aggregation and adsorption on the membrane surface. Through static and dynamic adsorption tests, the adsorption of the solute was tried to correlate with fl-FFF. As various membranes were used for the accumulation wall of the fl-FFF tested, this could simulate solute behavior in membrane filtration under similar chemical and hydrodynamic operating conditions. Thus, the fl-FFF system can be used to simulate actual membrane filtration with various solutes such as NOM in order to predict membrane performance for solutes (an earlier elution time for a certain solute with a membrane implies less fouling propensity and greater removal capability for the system).

Key words | flow field-flow-fractionation (fl-FFF), membrane fouling, NOM

Jihee Moon
Jaeweon Cho (corresponding author)
Department of Environmental Science and Engineering,
Gwangju Institute of Science and Technology (GIST),
1 Oryong-dong, Buk-gu, Gwangju 500-712,
Korea
Tel:+82 62 970 2443
Fax: +82 62 970 2434
E-mail: *jwcho@gist.ac.kr*

Do Hee Kim
Department of Second Chemistry,
Taean Thermal Power Plant,
Korea Western Power Co., Ltd,
831 Bang-gal Li, Won-buk Myun, Taean City,
Chungchungnamdo 357-910,
Korea

INTRODUCTION

The membrane filtration process has been recognised as one of many effective technologies for wastewater reclamation due to its good performance, especially for the removal of inorganic/organic micro-pollutants and wastewater effluent organic matter (EfOM). Despite this, one of the major impediments to the widespread application of the membrane filtration process in wastewater reclamation is membrane organic fouling (Ghayeni *et al.* 1998). In the operation of a membrane system, fouling may be influenced by membrane properties, feed water characteristics and hydraulic conditions of the system. Membrane organic fouling can be described as a result from the following mechanisms: (a) accumulation of a solute near the membrane surface, (b) gradual irreversible changes to the concentration polarisation layer and (c) adsorption or precipitation of a solute on the membrane surface. In particular, irreversible fouling is related to the adsorption and precipitation of organic or inorganic compounds on the membrane surface or within pores (Kim *et al.* 1992; Jucker & Clark 1994). Therefore, membrane fouling due to solute adsorption on or within the membrane should be rigorously characterised to evaluate and predict the membrane's performance.

The separation of macromolecular materials, both for preparative and analytical purposes, has become one of the most demanding activities for separation scientists

worldwide. For membrane filtration processes, the size distribution of natural organic matter (NOM) and colloids is one of the most influencing factors in terms of removal efficiency and membrane fouling. There are various analytic methods to determine the sizes of the molecules such as UF separation, HPLC-SEC, dynamic laser light scattering and ultrasonic spectroscopy. Flow field-flow-fractionation (fl-FFF) is one method by which the size distribution of particles, macromolecules and colloidal materials in water can be determined (Dulod & Sachauer 1996; Hecker *et al.* 1999; Gidding 1989). One of the advantages of the fl-FFF technique is that fl-FFF is able to efficiently determine particle sizes without a calibration with theoretical equations (Dulod & Sachauer 1996; Schure 1999). Equation (1) exhibits the relationship between retention time and particle size for asymmetric fl-FFF:

$$t_r = \frac{\pi\eta w}{2kT}\ln\left[\left(\frac{Z}{L} - \frac{V_c + V}{V_c}\right)\Big/\left(1 - \frac{V_c + V}{V_c}\right)\right]d \qquad (1)$$

where t_r is the retention time, η is the viscosity, w is the channel thickness, V_c is the cross-flow rate, k is the Boltzmann constant, T is the absolute temperature, V is the channel flow rate, d is the diameter, Z is the distance of the focusing point from the start of the channel and L is the channel length.

Fl-FFF is a separation technology similar to chromatography, and separation by fl-FFF is produced by a field defined as an external influence that is applied in a direction perpendicular to the channel flow (Schimpf *et al.* 2000). Fl-FFF employs a membrane as the accumulation wall and the field of fl-FFF is a cross-flow of fluid in a carrier solution (Hartmann & Williams 2002); thus particles with varying sizes and diffusion coefficients are separated inside the channel. After an injection, it is affected by the parabolic velocity profile across the channel as well as by the cross-flow. Smaller particles are diffused back further into the channel than larger particles because of their higher diffusion coefficients. Consequently, smaller particles are located in a faster channel flow stream; thus, they can be eluted faster than larger particles located in slower streamlines. This characteristic of fl-FFF makes it possible to evaluate the physicochemical interaction between membrane and solutes such as NOM and EfOM. Thus, fl-FFF can provide a useful means for investigating membrane fouling with EfOM, even though FFF is traditionally used for the measurement of molecular weight and particle size distribution. Using this characteristic of fl-FFF, the interaction between membrane properties and the NOM size, and related membrane fouling behavior are expected to be evaluated.

The objectives of this study are to investigate and demonstrate the effects of ionic strength on solute behavior in membranes and to correlate membrane fouling with fl-FFF.

HYPOTHESES

The first hypothesis of this study is on the chemistries of the eluent (or carrier), whose pH and ionic strength influences the separation behavior of the solute during fl-FFF operation. According to the basic fl-FFF theory, the velocity of the solute in the channel is affected by diffusion and crossflow forces (see Figure 1(a)). In addition, the retention time of a solute increases with increasing size of the solute because diffusivity of the solute decreases and cross-flow force increases with increasing solute size. In this study, we changed the ionic strength of the carrier solution and used both charged and non-charged membranes, so the velocity of the solute in the channel can be affected by the membrane charge and ionic strength of the carrier (see Figure 1(b)). We hypothesised that the increase of ionic strength can make solutes come closer to the bottom of

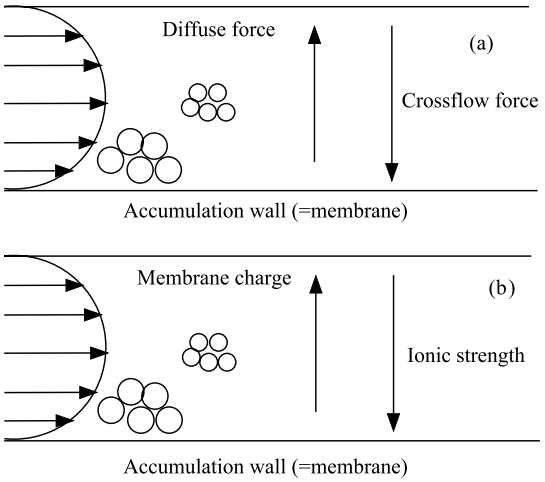

Figure 1 | The basic separation principle for the fl-FFF (a) and related hypotheses (b).

the channel due to the compaction of a double layer, and retention time increases.

Therefore, transport and removal mechanisms for solutes in membrane can be demonstrated by fl-FFF. The second hypothesis is that the fl-FFF fractogram of a solute is correlated with membrane fouling and the adsorption of the solute on the membrane surface (i.e. accumulation wall).

MATERIALS AND METHODS

Apparatus

An asymmetric fl-FFF system with a UV detector (AF 4 from Post Nova, Germany) was used. The channel has a length of 30 cm, a width of 4 cm and a thickness of 250 μm. As an accumulation wall, three different types of membranes were employed: (1) regenerated cellulose membranes (Aqua: MWCO of 1,000 and 10,000 Da, Post Nova, Germany), which are relatively hydrophilic and non-charged (i.e. least negatively charge) membranes, (2) a NF membrane (HL: MWCO of 250 Da, polyamide thin-film-composite (TFC), Desal, USA) and (3) a UF membrane (GM: MWCO of 8,000 Da, polyamide TFC, Desal, USA). Both HL and GM membranes have a highly negative surface charge in terms of the zeta potential at pH 7, which was measured by the electrophoresis method using a commercial apparatus (ELS-8000, Otsuka, Japan) as −9.90 mV and −20.00 mV, respectively (Shim *et al.* 2002). A goniometer (CAM-PLUS, Tantec, USA) was used to measure the contact angle of the membrane surface, which is a measure of the relative hydrophobicity of the membrane surface. The contact angle of the membrane was measured by a sessile drop method, which is based on the interacting angles between water, the membrane surface and air. Detailed properties of membranes are listed in Table 1.

Characteristics of feed and carry solutions

A phosphate buffer (pH 6.8) was used as a carrier solution for fl-FFF and the ionic strength of the carrier solution was adjusted to 10 mM and 100 mM with NaCl to demonstrate the effect of ionic strength on the retention time of either macromolecules, NOM,or EfOM. Moreover, the effect of the carrier solution was also investigated using a 0.1% sodium dodecyl sulfate (SDS: Sigma, USA) solution. As solutes for both membrane fouling and fl-FFF experiments, Suwannee River NOM (SR-NOM, International Humic Substance Society (IHSS), Golden, USA) and Nakdong River NOM (NR-NOM) were tested. NR-NOM was concentrated by a RO membrane (SN, Saehan, Korea) from the Nakdong River in Korea. The Nakdong River contains approximately 50% of effluent from various wastewater treatment plants. The concentrations of all NOM samples were adjusted to approximately 25 mg/L based on total organic carbon (TOC).

Conditions of bench scale membrane tests

The molecular weight distributions for both SR-NOM and NR-NOM were analysed using high performance size exclusion chromatography (HP-SEC) (Chin *et al.* 1994) and the two NOM had weight-averaged molecular weight (MW) values of 1,600 and 3,400 Da, respectively. Isolated NR-NOM was also used for comparison purposes with

Table 1 | Membrane properties

Membrane	Material	MWCO (Da)	Zeta potential (mV) @ pH 7.0	PWP (L/d m^2 kPa)	Contact angle (°)
GM	Polyamide TFC	8,000	−20.04	4.34	61.0
Aqua	Regenerated	10,000	−0.34	N.A.*	17.1
	Cellulose	1,000			
HL	Polyamide TFC	250	−9.90	3.35	63.0

*N.A.: not analysed.

different carrier solutions. Isolation of NOM was conducted with XAD-8/4 resins for the fractionation of hydrophobic (HP) and transphilic (TL) NOM and a dialysis membrane (regenerated cellulose, MWCO of 3,500 Da, Spectra, USA) for colloidal NOM (COM, i.e. having a molecular weight higher than 3,500 Da by technical definition) separation. Polystyrene sulfonates (PSS) with MW of 18,000 and 35,000 Da were also used in fl-FFF for comparison with NOM. Static and dynamic adsorption tests were conducted to investigate physicochemical interactions between the membrane and NOM/EfOM. The HL membrane was employed for adsorption tests; static adsorption tests were conducted using a diffusion cell (a membrane equipped between two chambers) having an active membrane area of 13.2 cm^2 over 24 h. Various different concentrations of NOM were applied. In addition, dynamic adsorption tests were also performed with membrane filtration units. For filtration tests, a bench-scale unit with a flat sheet membrane was used under the same hydrodynamic operating conditions determined from an initial J_0/k ratio of 1.0 (Cho *et al.* 2002*a*,*b*); J_0 (the initial pure water permeation flux (Equation (2)) and k (the back-diffusional mass transfer coefficient) can be calculated from the following equations (Mulder 1996)

$$J_0 = \frac{Q_p}{A_m} \tag{2}$$

$$k = 1.62\left(\frac{UD^2}{d_h L}\right)^{0.33} \quad (\text{thin-channel-type module}). \tag{3}$$

Here, Q_p and A_m are the permeate flow rate (cm^3/s) and membrane surface area (cm^2), respectively. Equation (2) is derived from the Sherwood number ($Sh = kd_h/D$) with consideration of the module configuration (flow regime), where U is the average velocity of the feed fluid (cross-flow velocity (cm/s)), D is the diffusion coefficient of the solute (cm^2/s) estimated by the Stokes–Einstein relationship, d_h is the equivalent hydraulic diameter (cm) and L is the channel length (cm).

The J_0/k ratio was obtained with deionized (DI) water, prior to the actual tests with NOM-containing feed waters. A particular initial J_0/k ratio was adjusted by varying J_0 (controllable by changing the transmembrane pressure) for a fixed value of k (changeable by varying the cross-flow velocity) or vice versa. Based on this pre-determined J_0/k ratio, membrane filtration tests were performed with those feed waters and membranes of interest. All of the filtration experiments were conducted in the recycle mode. Either reversible or irreversible NOM was desorbed into 0.1 N NaOH solution for one day after the flux reached a steady state. Correlation between adsorption tests and fl-FFF fractogram was identified by gradually decreasing cross-flow of fl-FFF after approximately 350 s.

RESULTS AND DISCUSSIONS

Effects of ionic strength of carrier solution

Figures 2(a) and (b) exhibit the effect of ionic strength on the elution peak and recovery of PSS 18,000 Da for a HL membrane at cross-flow values of 0.1 and 0.23 mL/min (1.39×10^{-5} and 3.19×10^{-5} cm/s), respectively; here, the relative fraction (i.e. y axis) is a fraction calculated based on the total chromatograph area being 1.0. In the ionic strength range of 1 and 10 mM, the earlier elution peak was observed at the lower ionic strength as expected from the hypotheses. However, for ionic strength values between 10 mM and 100 mM, the earlier and sharper peaks were observed at the higher ionic strength. The higher ionic strength was hypothesised to make PSS come closer to the accumulation wall (i.e. membrane) due to compaction of a double layer and retention time increases. A broad peak can also be expected because charged particles aggregate on the membrane surface more easily under a higher ionic strength condition. However, we observed a sharper peak and earlier retention time at a higher ionic strength (i.e. 100 mM). These unexpected results were probably caused by the shape of the PSS polymer. The shape of the PSS polymers depends on the solvent properties such as ionic strength (Manh *et al.* 2000). At a lower ionic strength, PSS presumably exhibits a rod-like structure and its shape changes to more coiled structures (i.e. higher with respect to the diffusion coefficient) as the ionic strength further increases. The coiled and compact structures of PSS can result in an earlier elution peak from fl-FFF measurement because those structures can provide smaller sizes than a linear structure. Figure 3 exhibits the effect of ionic strength

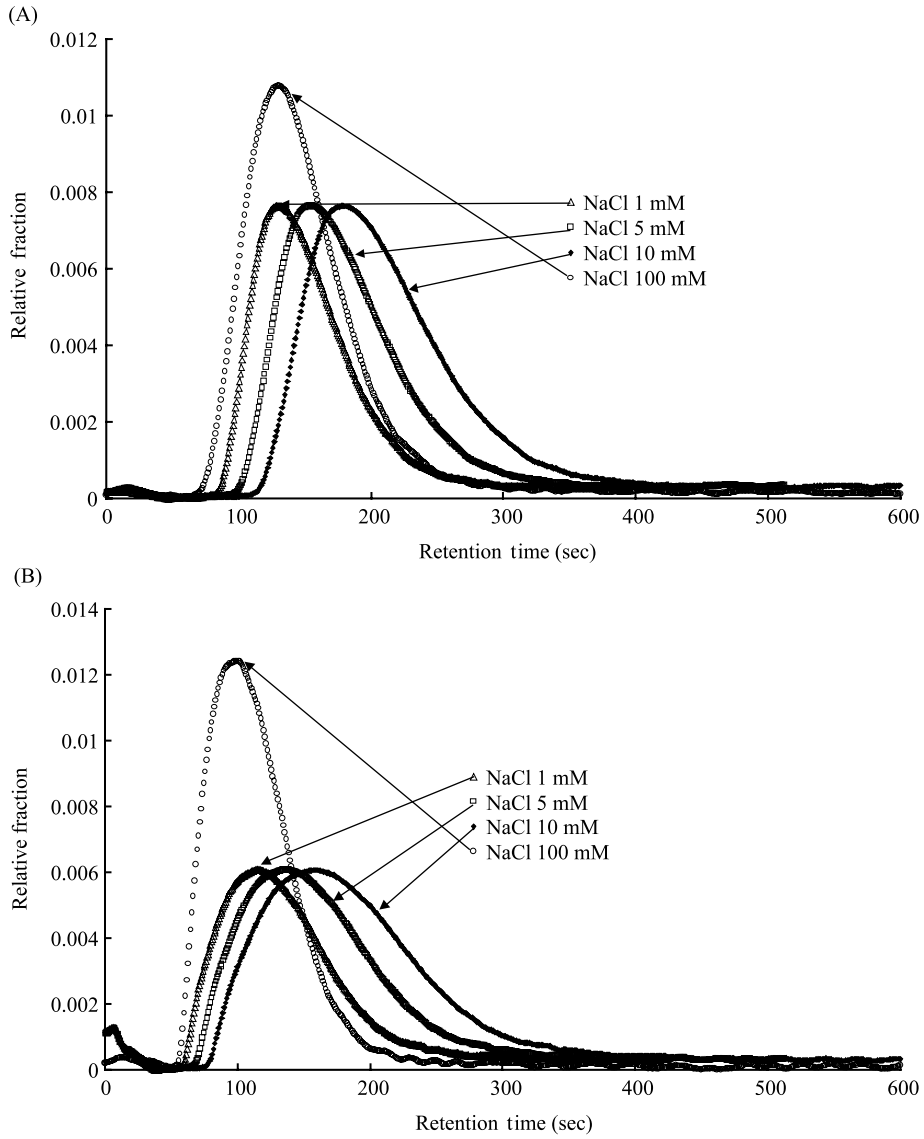

Figure 2 | The effect of ionic strength on retention time of PSS 18,000 Da demonstrated with a HL membrane: (A) cross-flow of 0.1 mL/min (1.38×10^{-5} cm/s) and a channel flow of 0.1 mL (0.17 cm/s), (B) cross-flow value of 0.23 mL/min (3.19×10^{-5} cm/s) and a channel flow of 0.1 mL (0.17 cm/s).

on the elution peak and recovery of PSS 18,000 Da for the Aqua membrane (i.e. least negatively charged) at a cross-flow of 1.9 mL/min (2.64×10^{-4} cm/s) and a channel flow of 0.10 mL/min (0.17 cm/s), respectively. Similar to the results with a HL membrane, at a low ionic strength range (1–10 mM), the earlier elution peak was also observed at lower ionic strengths due to reduced electrostatic repulsion between the membrane surface and PSS. The elution time of the peak at an ionic strength of 100 mM was somewhat different from that obtained with the HL membrane, but the shapes at an ionic strength of 100 mM for both membranes are similar. From the observed shapes for both membranes, it can be envisioned that the PSS becomes more coiled and compact (i.e. smaller in size) and its interaction with the membranes is minimised at an extremely high ionic strength (i.e. at 100 mM).

Figure 4 exhibits the effect of ionic strength on the elution peak and recovery of the two tested NOMs for a HL membrane at a cross-flow of 0.23 mL/min (3.19×10^{-5} cm/s) and a channel flow of 0.1 mL/min (0.17 cm/s), respectively. Table 2

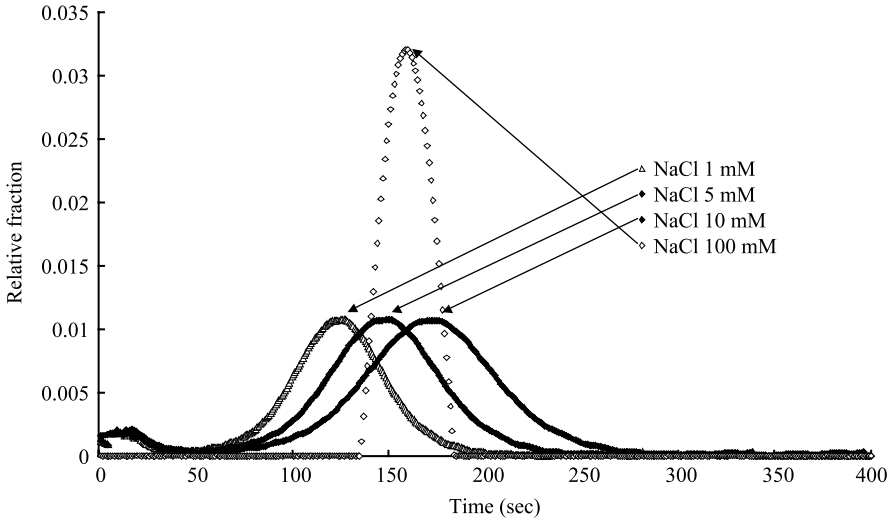

Figure 3 | The effect of ionic strength on retention time of PSS 18,000 Da demonstrated with the Aqua membrane (MWCO of 10,000 Da): cross-flow of 1.9 mL/min (2.64×10^{-4} cm/s) and a channel flow of 0.1 mL (0.17 cm/s).

summarises the total areas of the chromatogram calculated with the same baseline. The same trends were observed for both SR-NOM and NR-NOM, as shown in Figure 4. As found with PSS, both NOM represented earlier elution peaks at a high ionic strength. It can also be explained by structural changes depending on the ionic strength. Braghetta *et al.* (1997) reported the effect of ionic strength on the membrane matrix and suggested the conceptual model of molecular coiling and uncoiling depending on solution chemistry. At a higher ionic strength, membrane polymers are getting closer to each other and more compact and charged membranes have a reduced diffusion double layer. Likewise, NOM may exhibit a more compact, rigid and coil-shaped structure at a higher ionic strength. Distinguishable sharper and higher peaks were obtained at a higher ionic strength for NR-NOM and peaks for both NR-NOM and SR-NOM were obtained at earlier retention times than those at a lower ionic strength, as shown in Figure 4.

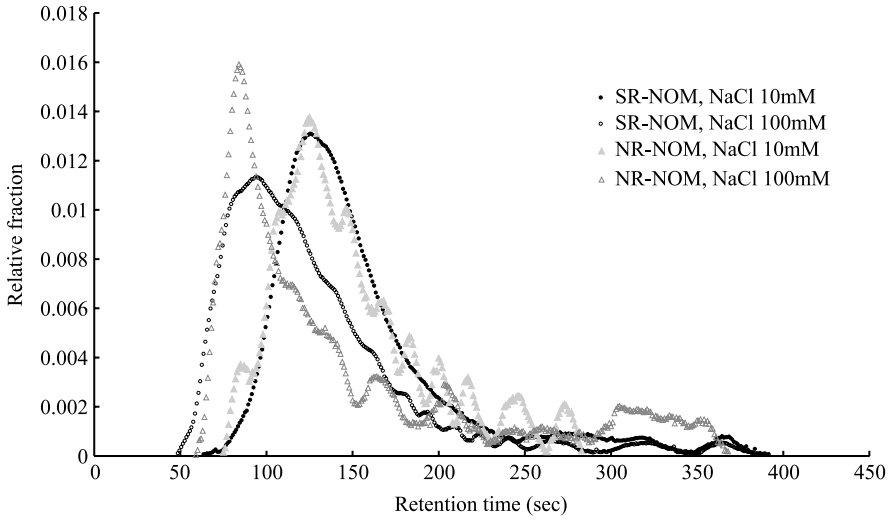

Figure 4 | Demonstration of ionic strength effects on the retention time of SR-NOM and NR-NOM for a HL membrane with cross-flow of 0.23 mL/min (3.19×10^{-5} cm/s) and a channel flow of 0.1 mL/min (0.17 cm/s).

Table 2 | Fractogram areas for SR-NOM and NR-NOM with different membranes

	GM (MWCO of 8,000 Da)		Aqua (MWCO of 10,000 Da)	
	Hydrophobic NOM	Transphilic NOM	Hydrophobic NOM	Transphilic NOM
Fractogram area	26.40	48.30	2.50	3.20

Effects of the membrane surface charge on NOM separation by fl-FFF

Figure 5 exhibits the effect of the membrane surface charge on the separation of NOM by the GM (MWCO of 8,000 Da) and the Aqua (MWCO of 10,000 Da) membranes at a cross-flow of 1.9 mL/min (2.64×10^{-4} cm/s) and a channel flow of 0.1 mL/min (0.17 cm/s), respectively. These two membranes contain similar pore size distributions. However, the GM membrane has a more negative surface charge than the Aqua membrane (see Table 1). The results showed the GM membrane separates both HP-NOM and TL-NOM successfully, but it is difficult to find any peak in the fractogram of the Aqua membrane. In addition, the total areas of both HP-NOM and TL-NOM for the GM membrane were approximately 10 times higher than those for the Aqua membrane (see Table 2). These results can be explained by the surface charge difference between the GM and Aqua membranes. The NOM molecules are smaller than the pores of the two membranes. Thus most parts of the NOM molecules could pass through the membrane pores. However, in the case of the GM membrane, the negatively charged membrane surface probably prevents NOM transmission into the membrane pores.

Figure 6 exhibited a UV fractogram for PSS with MW of 35,000 Da when two different membranes were employed as an accumulation wall in fl-FFF; virtually non-charged regenerated cellulose membranes (Aqua with MWCO of 1,000 and 10,000 Da) and highly negatively charged membranes (HL and GM) were tested. Both the HL and GM membranes provided earlier elution peaks than the non-charged regenerated cellulose membranes due to the membrane surface charge. The carrier is a phosphate buffer solution with a pH of 6.8, and both the HL and GM membranes have a negative surface charge at a pH of 6.8 in terms of zeta potential values, as measured by the electrophoresis method. Thus, electrostatic interaction between the membrane surface and PSS enables PSS to be placed away from the membrane surface, resulting in faster retention times for PSS.

Effects of various carrier solutions on NOM separation by fl-FFF

The effect of the carrier solution on the NOM separation by fl-FFF was demonstrated using 0.1% SDS and 10 mM NaCl

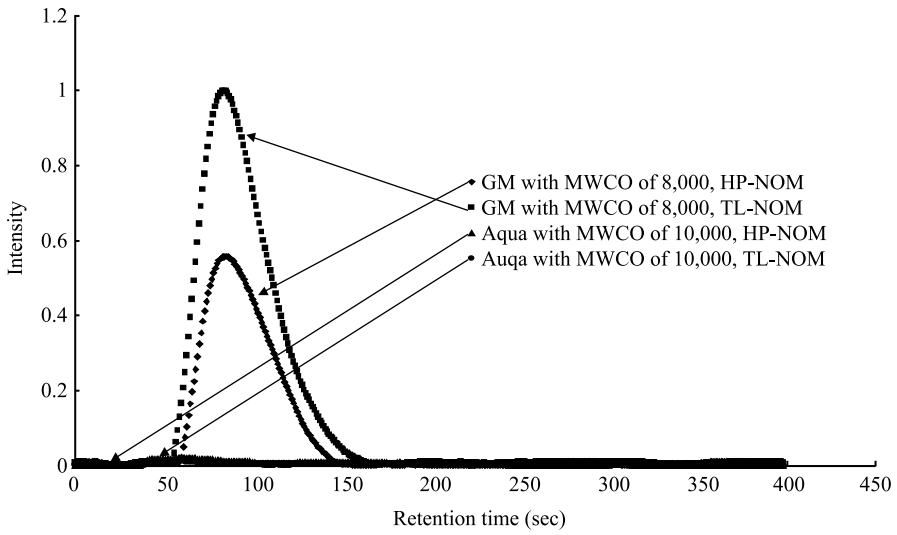

Figure 5 | Demonstration of the effects of the membrane surface charge on retention time of NR-NOM for GM and Aqua membranes with cross-flow of 1.9 mL/min (2.64×10^{-4} cm/s) and a channel flow of 0.1 mL/min (0.17 cm/s) (at an ionic strength of 10 mM and pH of 6.8–6.9).

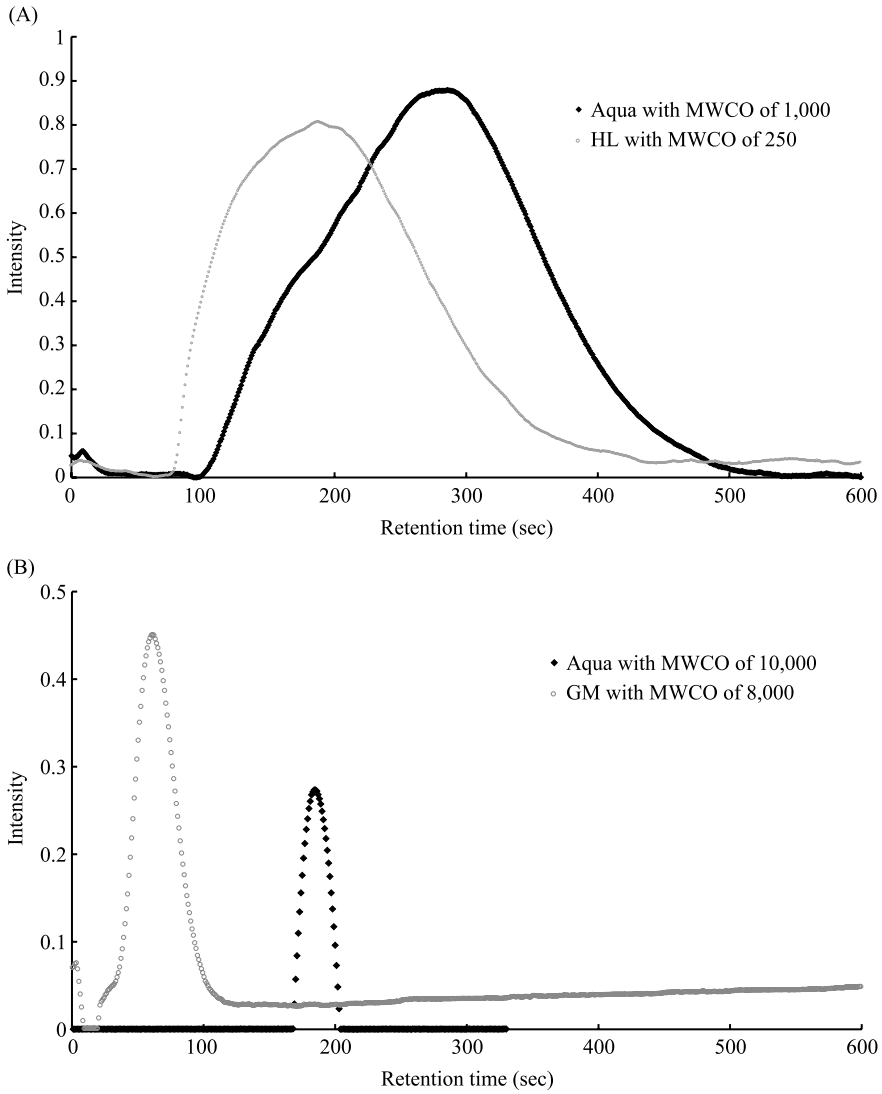

Figure 6 | UV fractogram for PSS with MW of 35,000 Da with different membranes: (A) the regenerated cellulose membrane (Aqua) with MWCO of 1,000 Da versus a HL membrane with MWCO of 250 Da at a cross-flow of 0.23 mL/min (3.19×10^{-5} cm/s), a channel flow of 0.1 mL/min (0.17 cm/s) and an ionic strength of 10 mM NaCl, and (B) Aqua with MWCO of 10,000 Da versus GM with MWCO of 8,000 Da, at a cross-flow of 1.9 mL/min (2.64×10^{-4} cm/s), a channel flow of 0.1 mL/min (0.17 cm/s) and an ionic strength of 100 mM NaCl.

solution, as shown in Table 3 and Figure 7. Various PSS with different molecular weights were tested, and retention time results for PSS with NaCl carrier solution provided relatively high differences among PSS with different molecular weights. Contrary to the NaCl solution, elution peaks for the SDS solution were almost similar. Similarly, there is virtually no difference in retention time between isolated NOM fractions for the SDS carrier solution, as shown in Figure 7. This can be explained by the effect of SDS; the negatively charged surfactant layer near the membrane surface becomes thicker due to the accumulation of anionic surfactant. Thus the subsequent parabolic velocity profile can influence retention time to a lesser extent.

Effect of characteristics of NOM on membrane fouling (in terms of NOM adsorption on the membrane surface)

Different NOM characteristics and their interaction with the membrane surface can affect membrane performance in

Table 3 | Retention times of various PSS with NaCl 10 mM and 0.1% SDS solution, and a HL membrane

PSS MW (Da)			1,800	4,600	8,000	18,000	35,000
Retention time (s)	Cross-flow of 0.1 mL/min (1.39×10^{-5} cm/s)	10 mM NaCl	166	169	176	178	186
		0.1% SDS	172	174	176	177	178
	Cross-flow of 0.23 mL/min (3.19×10^{-5} cm/s)	10 mM NaCl	124	128	132	158	188
		0.1% SDS	125	127	130	133	139

terms of fouling. Static adsorption tests for SR-NOM and NR-NOM with a HL membrane were conducted, as shown in Figure 8. A higher adsorbability was observed for SR-NOM than NR-NOM under the same pH and ionic strength conditions. Dynamic adsorption through membrane filtration tests with a HL membrane also evaluated the adsorbable properties of both SR-NOM and NR-NOM. Membrane filtration tests with both NOM were also performed until they reached a steady state after approximate 17 h. Both SR-NOM and NR-NOM exhibited an almost similar flux decline trend with a flux reduction percentage of 7%, but a higher removal efficiency and more desorbed NOM from a fouled HL membrane with SR-NOM were observed, as shown in Table 4.

These dynamic and static adsorption tests were tried to be correlated to the fl-FFF results; Figure 9 is expected to exhibit this correlation. After 350 s, cross-flow was gradually reduced and maintained at an almost zero flow rate. After cross-flow was reduced and almost terminated, another elution peak then appeared. This elution peak without cross-flow is believed to represent either adsorbed NOM on, or accumulated NOM near, the membrane surface. As shown in Figure 9, elution peaks appear after terminating the cross-flow, but the shape of these elution peaks seem fractogram tails rather than peaks. Thus, the amount of either adsorbed or accumulated NOM on the membrane surface in terms of fouling could not be quantitatively evaluated.

CONCLUSIONS

Chemical interactions between the membrane surface and NOM were demonstrated using the fl-FFF system with

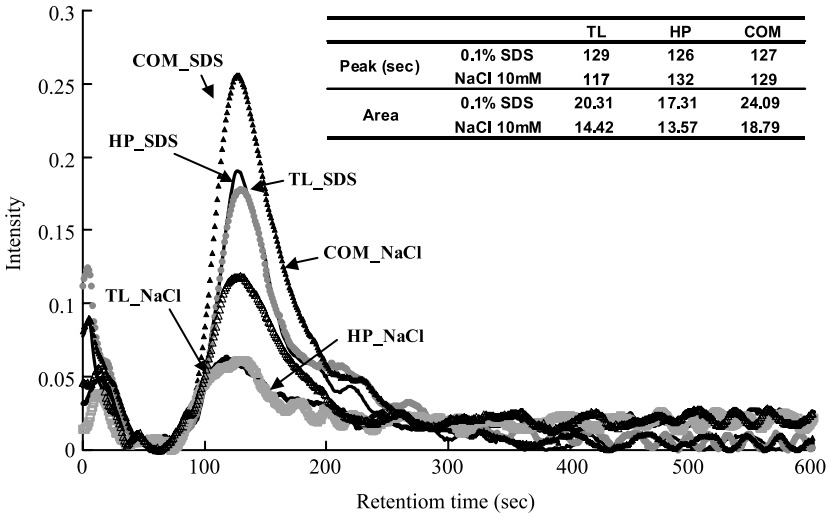

		TL	HP	COM
Peak (sec)	0.1% SDS	129	126	127
	NaCl 10mM	117	132	129
Area	0.1% SDS	20.31	17.31	24.09
	NaCl 10mM	14.42	13.57	18.79

Figure 7 | UV chromatogram of isolated NR-NOM (hydrophobic, transphilic and colloidal NOM constituents) for SDS 0.1% and NaCl 10 mM carrier solution.

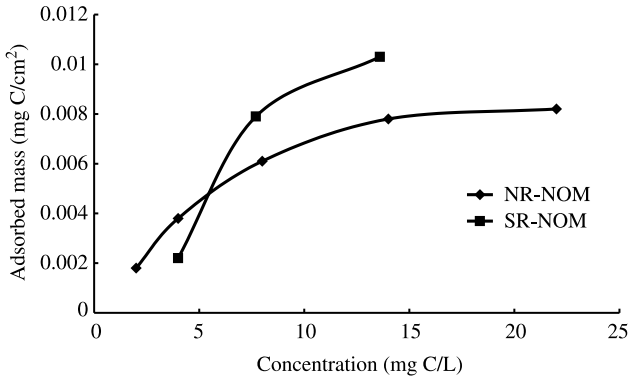

Figure 8 | Static adsorption of SR-NOM versus NR-NOM for the HL membrane.

Table 4 | Dynamic adsorption results obtained through filtration tests with the HL membrane

	Reduced permeability ratio, P/P_0 (%)	Removal efficiency (%)	Desorbed NOM (mgC/cm^2)
SR-NOM	6.2	94.4	0.013
NR-NOM	7.6	90.9	0.008

different membranes containing different surface charges, with respect to electrostatic interaction and solute structure changes. To demonstrate the effect of ionic strength during membrane filtration, different ionic strengths were applied on various solutes. The results showed that ionic strength was identified to affect both solute transport in the micro-channel of fl-FFF and adsorption or accumulation of solute on the membrane surface, by altering the molecular structure of the solute. The retention time in fl-FFF for PSS increases with increasing ionic strength as electrostatic repulsion between the membrane surface and PSS decreases. However, at an extremely high ionic strength, the retention time even decreases as the molecular structure of the tested solutes changes to a more coiled shape (thus, smaller in size). These trends were also identified as true for two different NOM obtained from natural waters. Thus, the ionic strength is one of the important factors in membrane fouling and solute removal. The membrane surface charge (in terms of the zeta potential) was one of the important factors affecting solute separation; the membrane charge always showed a positive effect on solute removal in this study. The anionic surfactant, SDS, could reduce the interval of retention time of NOM. Thus there were almost similar retention times even for different NOM with different molecular weights (however, it should be recalled that this phenomenon can be anticipated only with the surfactant (i.e. SDS)). As various membranes were used for the accumulation wall of the fl-FFF tested, this could simulate solute behavior in membrane filtration under similar chemical and hydrodynamic operating conditions. Thus, the fl-FFF system can be used to simulate actual membrane filtration with various solutes such as NOM in order to predict membrane

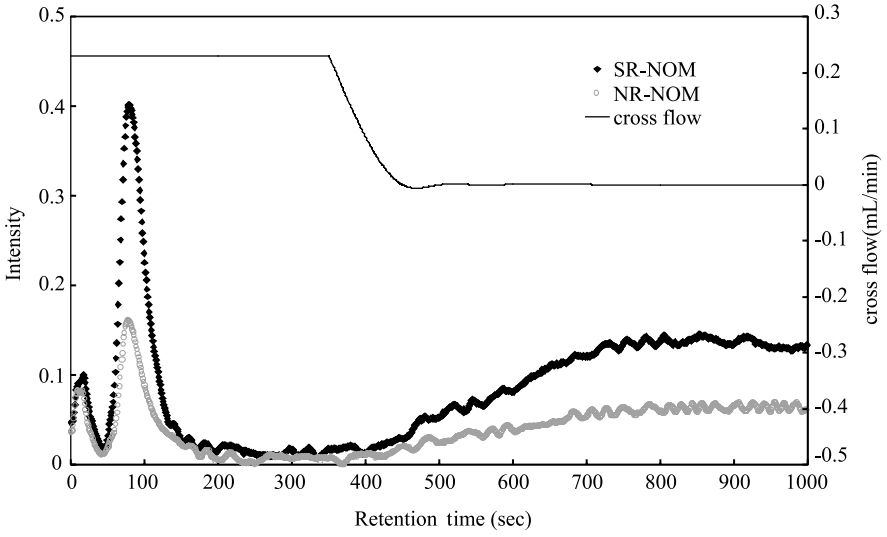

Figure 9 | UV fractograms of SR-NOM and NR-NOM with a HL membrane under gradually decreasing cross-flow condition (at an ionic strength of 10 mM and pH of 6.8–6.9).

performance for the solutes (an earlier elution time for a certain solute with a membrane implies a reduced fouling tendency and a greater removal capability, for example).

ACKNOWLEDGEMENTS

This work was supported by a grant (code 4-1-2) from Sustainable Water Resources Research Center of 21st Century Frontier Research Program, and also partly supported by the Center for Distributed Sensor Network at GIST.

REFERENCES

Braghetta, A., DiGiano, F. A. & Ball, W. P. 1997 Nanofiltration of natural organic matter: pH and ionic strength effects. *J. Environ. Engng., ASCE* **123**, 628–641.

Chin, Y. E., Aiken, G. & O'Loughlin, E. 1994 Molecular weight, polydiversity, and spectroscopic properties of aquatic humic substance. *Environ. Sci. Technol.* **28**, 1853–1858.

Cho, J., Amy, G., Jaeweon, Cho, Yoon, Y. & Sohn, J. 2002a Predictive models and factors affecting natural organic matter (NOM) rejection and flux decline in ultrafiltration (UF) membranes. *Desalination* **142**, 245–255.

Cho, J., Sohn, J., Choi, H., Kim, I. S. & Amy, G. 2002b Effects of molecular weight cutoff, f/k ratio, and hydrophobic interactions on NOM rejection and fouling in membranes. *AQUA* **51**(2), 21.

Dulod, L. & Sachauer, T. 1996 Field flow fraction of particle size determination. *Prog. Organic Coatings* **28**, 25–31.

Ghayeni, S. B., Beatson, P. J. & Fane, A. G. 1998 Water reclamation from municipal wastewater using combined microfiltration-reverse osmosis: preliminary performance data and microbiological aspects of system operation. *Desalination* **116**, 65–80.

Gidding, J. 1989 Field-flow-fractionation of macromolecules. *J. Chromatogr. A* **470**, 327–335.

Hartmann, L. & Williams, S. 2002 Flow field-flow-fractionation as an analytical technique to rapidly quantitate membrane fouling. *J. Membrane Sci.* **209**, 93–106.

Hecker, R., Fawell, R. D., Jefferson, A. & Farrow, J. B. 1999 Flow field-flow-fractionation of high-molecular-mass polyacrylamide. *J. Chromatogr. A* **837**, 39–151.

Jucker, C. & Clark, M. M. 1994 Adsorption of aquatic humic substances on hydrophobic ultrafiltration membranes. *J. Membrane Sci.* **97**, 37–52.

Kim, K. J., Fane, A. G., Fell, C. J. D. & Joy, D. C. 1992 Fouling mechanism of membranes during protein ultrafiltration. *J. Membrane Sci.* **68**, 79–91.

Manh, T., Geckeis, H. & Beck, H. P. 2000 Application of the fl-FFF to the characterization of aquatic humic colloids: evaluation and optimization of the method. *Colloids Surfaces A: Physicochem. Engng. Aspects* **181**, 289–301.

Mulder, M. 1996 *Basic Principles of Membrane Technology*, second edition. Kluwer Academic Publishers, Dordrecht.

Schimpf, M., Caldwell, K. & Giddings, J. 2000 The FFF family: underlying principles. In *Field-flow-fractionation Handbook*, Schimpf, M., Caldwell, K. & Giddings, J. C. (eds). Wiley, New York, pp. 3–30.

Schure, M. R. 1999 Advances in the theory of particle size distributions by field-flow fraction outlet and apparent polydiversity at constant field. *J. Chromatogr.* **831**, 89–104.

Shim, Y., Lee, H.-J., Lee, S., Moon, S.-H. & Cho, J. 2002 Effects of natural organic matter and ionic species on membrane surface charge. *Environ. Sci. Technol.* **36**, 3864–3871.

First received 16 January 2004; accepted in revised form 20 August 2004